Potts flux tube model at nonzero chemical potential

Jac Condella and Carleton DeTar
Department of Physics, University of Utah, Salt Lake City, Utah 84112
(Received 15 October 1999; published 7 March 2000)

We model the deconfinement phase transition in quantum chromodynamics at nonzero baryon number density and large quark mass by extending the flux tube model (three-state, three-dimensional Potts model) to nonzero chemical potential. In a direct numerical simulation we confirm mean-field-theory predictions that the deconfinement transition does not occur in a baryon-rich environment.

PACS number(s): 12.38.Aw, 05.50.+q, 64.30.+t

I. INTRODUCTION

The prospects of creating a quark-gluon plasma in the laboratory and interest in the role of such a plasma in the early Universe and in dense stars have stimulated efforts to understand the plasma–ordinary-matter phase transition starting from first principles in quantum chromodynamics (QCD). It is widely suspected that the phase transition occurs at high density as well as at high temperature. While much progress has been made in characterizing the phase transition at high temperature at zero average baryon density in full QCD, the same degree of success has not been achievable at nonzero density, chiefly because the standard SU(3) lattice action becomes complex, invalidating standard Monte Carlo methods. Simulations must then be carried out with related ensembles of real, positive weight. Studies on small volumes offer intriguing hints about the phase structure at nonzero density. But with the wrong ensemble, the thermodynamic limit cannot be taken, so the phase structure cannot be ascertained [1,2]. Thus we turn to simple statistical models for insight.

The three-dimensional three-state Potts model is one of the standard paradigms for lattice QCD in the strong-coupling, high-temperature, large-quark-mass limit [3–5]. It has been used to provide qualitative information about the deconfinement phase transition. Past Potts model studies have been limited to simulations at zero quark chemical potential and to mean-field studies at nonzero chemical potential. In this work we show that the Potts model can be extended easily to nonzero baryon chemical potential, permitting direct simulation using standard techniques.

The QCD phase transition changes character as the quark masses and flavors are varied. At zero quark mass with two or more flavors the transition restores the spontaneously broken chiral symmetry [6]. At infinite quark mass it leads to ''deconfinement'' in the pure Yang-Mills theory. Simulations of full QCD with two flavors at zero chemical potential show that these two regimes are separated at intermediate quark mass by a region where no phase transition occurs—only a strong crossover. In the corresponding Potts model we find this obliteration of the deconfinement transition, not only as the quark mass is lowered, but also as the chemical potential is increased. The former is found from direct simulation, but the latter has been known until now only in mean field theory [5]. Here we confirm the mean field prediction with a direct simulation.

Because the Potts model analogy works only in the large quark mass limit, we learn only the fate of the deconfinement transition and not the chiral transition. Nonetheless, to the extent that a strong crossover in QCD, observed in the intermediate quark-mass regime, is a vestige of deconfinement, one may speculate that a weakening of the QCD crossover at nonzero chemical potential is then indicated.

In the following section we describe the model. In Sec. III we present results of a simulation. A summary and discussion are offered in the final section.

II. MODEL

We use a variant of the flux tube model of Patel [4] also discussed in [7]. The model describes a classical statistical system with no dynamics, consisting of a three-dimensional cubic lattice with quarks and antiquarks occupying the sites and color flux tubes occupying the nearest-neighbor links. A configuration is characterized by the quark number distribution $n_r \in [-3,-2,\ldots,3]$ and the color flux $l_{r,i} \in [-1,0,1]$ for each lattice site r and associated links in the $i=1,2,3$ directions. For convenience links entering a site from a negative direction are denoted alternatively by $l_{r,-i}=l_{r-\hat{i},i}$. Gauss's law is enforced in modulo 3 arithmetic:

$$\sum_{i=1}^{3} (l_{r,i}-l_{r,-i}) = n_r \mod 3. \tag{1}$$

The Hamiltonian assigns a mass m to each quark and flux link energy σ to each link:

$$H=\sum_{r,i} \sigma|l_{r,i}| + \sum_{r} m|n_r|. \tag{2}$$

The grand canonical partition function at inverse temperature β and quark chemical potential μ is then

$$Z_f(\beta,\mu)=\sum_{\{l_{r,i},n_r\}}{}' \exp[-\beta(H-\mu N)] \tag{3}$$

where $N=\Sigma_r n_r$ and the prime indicates that the sum is over all configurations satisfying Gauss's law.

The model is strictly static. The lowest vacuum excitations consist of mesons built from a quark-antiquark pair separated by one flux link and baryons consisting of three quarks on a site. Further excitations lead to extended baryons and mesons and more complex hadrons, always of zero tri-

ality. (We limited quark occupation to a maximum of three per site, but do not expect qualitative changes in our results if we increase this limit.)

The flux tube model is equivalent to the three-state three-dimensional Potts model with complex magnetic field. That is, $Z_f \propto Z_p$, where the Potts model partition function is

$$Z_p = \sum_{z_r} \exp\left(\beta' J \sum_{r,i} \mathrm{Re}(z_r z_{r+i}^*) + \beta' h \sum_r \mathrm{Re}\, z_r + i\beta' h' \sum_r \mathrm{Im}\, z_r \right). \tag{4}$$

This is the form of the Potts model found from the high-temperature, high-quark-mass, strong-coupling limit of lattice QCD [3,5]. The equivalence is established by a change of basis. The derivation starts by replacing the Gauss's law constraint at each site by a Kronecker delta in mod 3:

$$\frac{1}{3} \sum_{z \in Z(3)} z^l = \delta_{l,0}. \tag{5}$$

When we introduce one such sum for each site in the lattice, the sums over link and site occupation numbers decouple and can be summed explicitly. The $Z(3)$ constraint variables z_r become the ''clock'' spins of the Potts model. After rearranging the sums we have

$$Z_f(\beta,\mu) = \sum_{z_r} \prod_{r,i} \left(\sum_{l_{r,i}} \exp(-\beta\sigma |l_{\mathbf{r},\mathbf{i}}|)(z_r z_{r+\hat{i}}^*)^{l_{\mathbf{r},\mathbf{i}}} \right) \times \prod_r \left(\sum_{n_r} \exp[-\beta(m|n_{\mathbf{r}}| - \mu n_{\mathbf{r}})] z_r^{-n_r} \right). \tag{6}$$

The sums under the product symbols are explicitly

$$1 + 2\,\mathrm{Re}(z_{\mathbf{r}} z_{\mathbf{r}+\hat{\mathbf{i}}}^*) \exp(-\beta\sigma) \tag{7}$$

$$1 + u^3 + v^3 + z(v^2 + u) + z^*(u^2 + v) \tag{8}$$

where

$$u = \exp[-\beta(m+\mu)] \quad \text{and} \quad v = \exp[-\beta(m-\mu)]. \tag{9}$$

With the aid of an identity over $Z(3)$ these factors can be rewritten in exponential form. The identity we need is

$$1 + az + bz^* = \exp(c + d\,\mathrm{Re}\, z + ie\,\mathrm{Im}\, Z) \tag{10}$$

where

$$3c = \ln(1 + a + b) + \ln(1 - a - b + a^2 + b^2 - ab) \tag{11}$$

$$3d = 2\ln(1 + a + b) - \ln(1 - a - b + a^2 + b^2 - ab) \tag{12}$$

$$\frac{\sqrt{3}}{2} e = \arctan\left(\frac{\sqrt{3}(a-b)}{2 - a - b} \right). \tag{13}$$

Applying this identity to the first factor (7) gives the relation between the Potts spin coupling and the string energy (in units of the respective temperatures),

$$J\beta' = \frac{2}{3} \ln\left(\frac{1 + 2\exp(-\beta\sigma)}{1 - \exp(-\beta\sigma)} \right), \tag{14}$$

and to the second factor (8), gives the relation between the Potts magnetic fields and the quark mass and chemical potential

$$h\beta' = \frac{2}{3}\ln(1 + a + b) - \ln(1 - a - b + a^2 + b^2 - ab) \tag{15}$$

$$h'\beta' = \frac{2}{\sqrt{3}} \arctan\left(\frac{\sqrt{3}(a-b)}{2 - a - b} \right) \tag{16}$$

where

$$a = \frac{v^2 + u}{1 + u^3 + v^3} \tag{17}$$

$$b = \frac{u^2 + v}{1 + u^3 + v^3}. \tag{18}$$

Notice that h' is odd in μ and h is even. At zero chemical potential the imaginary coupling vanishes ($h' = 0$) and at infinite quark mass the real field h also vanishes. In this limit the Potts model exhibits the well-known first order transition at a value $\beta_t' J = 0.36703(14)$, known from numerical simulation [8]. Here we have the Potts–flux-tube parameter equivalence

$$(\beta_t' J = 0.3670,\ \beta_t' h = \beta_t' h' = 0) \equiv (\beta\sigma = 1.6265,\ \beta m = \infty,\ \beta\mu = 0). \tag{19}$$

Numerical simulation has indicated that the first order transition persists to a small real magnetic field [5]. The critical endpoint is crudely known to be in the range $[0.002, 0.01]$ for which

$$(\beta' J = 0.365,\ \beta' h = [0.002, 0.01],\ \beta' h' = 0) \equiv (\beta\sigma = 1.632,\ \beta m = [3.2, 4.2],\ \beta\mu = 0). \tag{20}$$

Any mass m higher than this critical value should admit a first order phase transition.

We chose to simulate the flux tube model at quark mass $m/\sigma = 5$. This value was selected to assure a first order phase transition at zero chemical potential. Figure 1 shows the mapping from flux tube $\beta\sigma$ to Potts parameters at zero chemical potential. We then repeated the simulation at nonzero chemical potential $\mu/\sigma = 1.75$. The corresponding map is shown in Fig. 2. The Potts magnetic fields remain small.

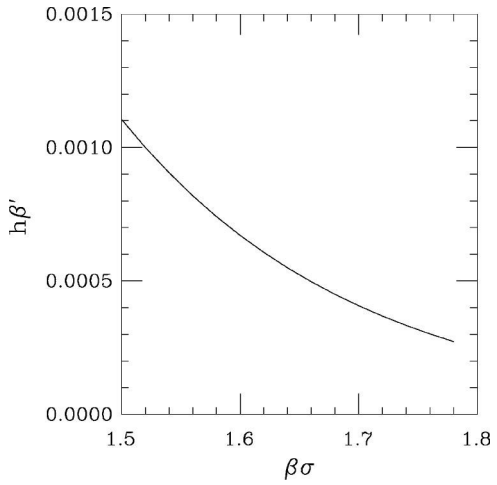

FIG. 1. Mapping of flux tube parameters $\beta\sigma$ to real Potts magnetic field $\beta' h$ at fixed quark mass $m/\sigma=5$ and zero chemical potential. A first order phase transition is expected at $\beta\sigma\approx 1.63$.

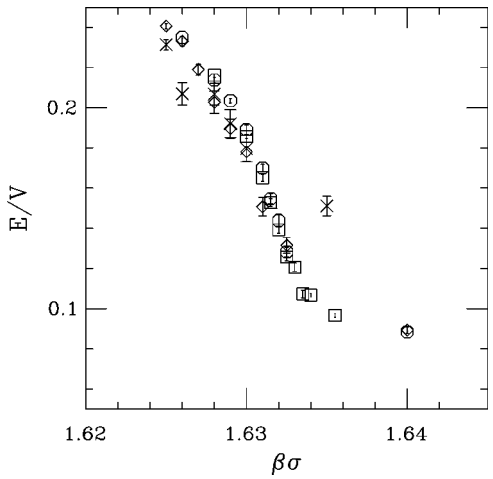

FIG. 3. Energy density vs $\beta\sigma$ in the critical region at zero chemical potential for various lattice sizes: $L=10$, crosses; 20, diamonds; 30, octagons; 40, squares.

III. METHOD AND RESULTS

We carry out a simulation in the occupation number basis (3), i.e. the flux tube formulation, in which the Boltzmann weights are real and positive and the simulation can be done easily using conventional Metropolis methods. We have chosen an elementary set of Metropolis moves that preserve the Gauss's law constraint, and are capable of reaching any valid configuration. The local moves consist of systematically ''adding'' or ''subtracting'' one of four elementary color-singlet hadrons at all locations and orientations in the configuration. A single sweep of the lattice consists of considering each of these moves for all orientations of the hadrons at each lattice site in typewriter order.

The Metropolis-move hadrons are these: (1) a quark and antiquark separated by one flux link, (2) a diquark and antidiquark separated by one flux link, (3) a quark and diquark or antiquark and antidiquark, also separated by one flux link, Eq. (4), and (4) a plaquette of flux links. The process of adding (or subtracting) a hadron consists of increasing or decreasing the quark occupation number and flux link value of the configuration in mod 3 arithmetic according to the position and orientation of the hadron selected, respecting our exclusion principle that limits the quark number to the range $[-3,3]$. By always adding or subtracting a color singlet state, Gauss's law is always obeyed. While all configurations satisfying Gauss's law can be reached by a combination of these moves, this over-complete set was also chosen in an effort to cover the phase space efficiently. Still, we have only a local algorithm, presumably as effective as a local algorithm in the spin basis. For the moment we have not considered cluster algorithms analogous to those that have been so successful in spin systems [9].

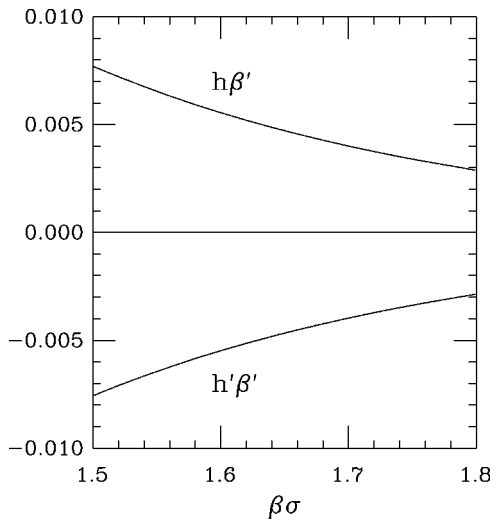

FIG. 2. Mapping of flux tube parameters $\beta\sigma$ to Potts real and imaginary magnetic fields $\beta' h$ and $\beta' h'$ at fixed quark mass $m/\sigma=5$ and nonzero chemical potential $\mu/\sigma=1.75$.

As we have mentioned we simulate at fixed quark mass $m/\sigma=5$ and choose two values of the chemical potential, namely $\mu/\sigma=0$ and 1.75. We then vary $\beta\sigma$ to locate the phase transition or crossover. We expect to reproduce the Potts first order phase transition at zero chemical potential and small real field, but at nonzero chemical potential we explore new territory. We simulate at a series of volumes L^3 for $L=10,20,30,40$ in each case. In the crossover region we extend the simulations for, typically, 35000–60000 Metropolis sweeps.

As expected at zero chemical potential, we find a sharp rise in energy density at $\beta\sigma\approx 1.63$ as shown in Fig. 3. To characterize the phase transition we study the size dependence of the peak in specific heat [10]. The specific heat is defined in the usual way in terms of the total energy E of the configuration:

$$C_V/\beta^2=(\langle E^2\rangle-\langle E\rangle^2)/L^3. \tag{21}$$

Figure 4 shows a peak in the specific heat at zero chemical potential that sharpens and grows with increasing volume. Also shown in these figures are results of a fit to a phenomenological form for a first order phase transition

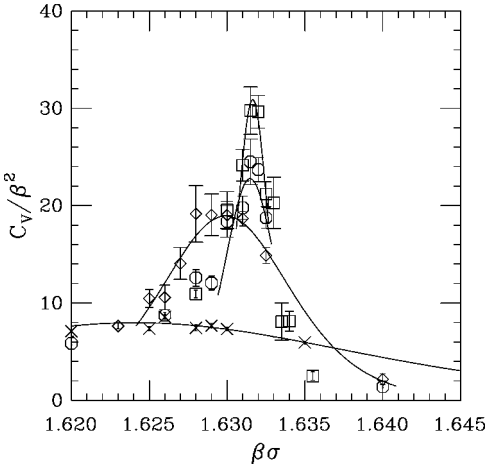

FIG. 4. Specific heat vs $\beta\sigma$ at zero chemical potential for various lattice sizes. Symbols as in Fig. 3.

based on a simplification of the finite size analysis of Borgs *et al.* [11]:

$$C_V/\beta^2 = \frac{C_{V,\max}(L)}{\cosh^2[\,\gamma(L)(\beta-\beta_c(L))]}. \tag{22}$$

The simplification assumes that the probability distribution for the energy density near the phase transition receives a delta function contribution from the two phases with the usual Boltzmann weights:

$$P(E) \propto \delta(E-E_d)\exp(-\beta E_d + S_d) + \delta(E-E_o)\exp(-\beta E_o + S_o) \tag{23}$$

in terms of the energy and entropy in the ordered and disordered phases. This model gives

$$\gamma = L^3 Q/2 \tag{24}$$

$$C_{V,\max} = L^3 Q^2/4 \tag{25}$$

for $Q=(E_d-E_o)/L^3$, the latent heat of the transition. In fact the actual probability distribution resembles a sum of broad peaks, but since we are concerned only with extracting $C_{V,\max}$, it suits our purpose. Although there are really only two independent parameters, β_c and Q, we have kept the height, width, and center unconstrained and look for evidence for scaling with L^3.

In Fig. 5 we plot the specific heat maximum vs L^3 and show that a linear relationship is plausible for $L \geq 20$. Errors are obtained using a bootstrap method, averaging simulation results in blocks, and extrapolating to infinite block size. Departures from linearity for smaller L are well known in this model and arise from finite size effects. We take the approximate scaling of the peak in specific heat as good evidence for a first order phase transition.

The quark number susceptibility (three quarks = one baryon), defined as

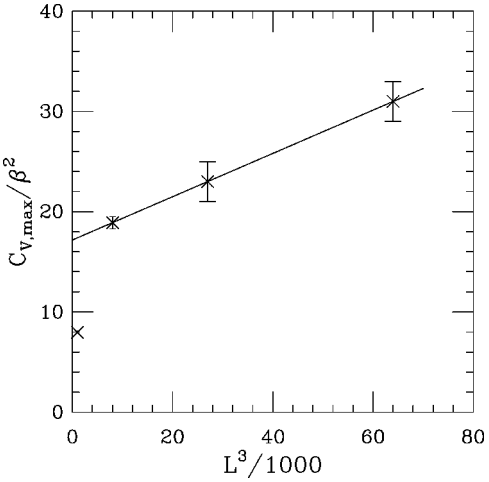

FIG. 5. Peak in specific heat vs lattice volume at zero chemical potential.

$$\chi_q = \frac{dB}{d\mu} = 9(\langle B^2\rangle - \langle B\rangle^2)/L^3 \tag{26}$$

with $B=\langle \Sigma_r n_r/3\rangle$, the total baryon number, rises as the temperature is increased past the phase transition, as shown in Fig. 6.

Having tested the method, we turn to nonzero chemical potential. Shown in Fig. 7 is a plot of the energy density vs $\beta\sigma$. We see evidence for a weak crossover. Notice that here and in the remaining figures, we have enlarged the $\beta\sigma$ scale compared with the corresponding zero chemical potential figures. Thus the crossover is far less abrupt than at zero chemical potential. The corresponding specific heat is shown in Fig. 8. There is a diffuse peak in the specific heat, but we see no evidence that the peak height is changing with increasing volume. The peak height is considerably smaller than at zero chemical potential, consistent with a broadening of the crossover. Thus we find no evidence of a phase transition at this chemical potential and quark mass.

We turn to the quark number density and susceptibility. Figure 9 shows the quark number density as a function of $\beta\sigma$. We note that in the high temperature range, the quark number density at our chosen mass is quite low—namely,

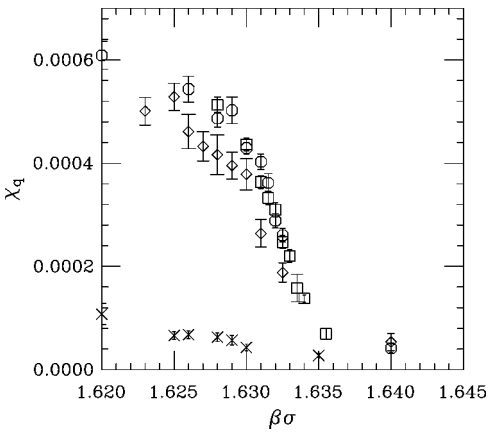

FIG. 6. Quark number susceptibility vs $\beta\sigma$ at zero chemical potential for various lattice sizes. Symbols as in Fig. 3.

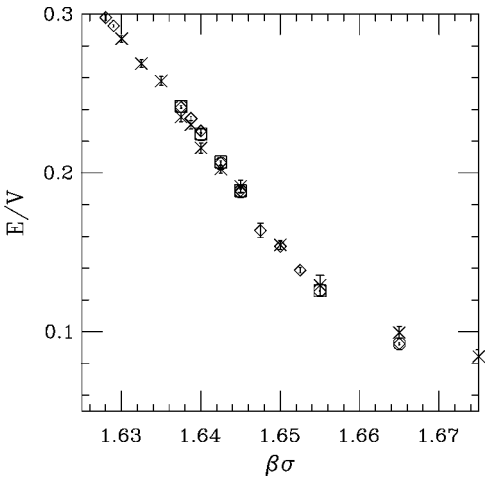

FIG. 7. Energy density vs $\beta\sigma$ at chemical potential $\beta\mu = 1.75$ for various lattice sizes. Symbols as in Fig. 3.

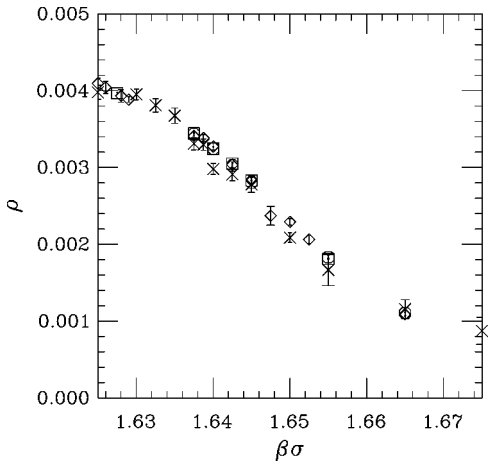

FIG. 9. Quark number density vs $\beta\sigma$ at chemical potential $\beta\mu = 1.75$ for various lattice sizes. Symbols as in Fig. 3.

only a few per thousand sites. The density rises as temperature is increased past the crossover. As with the energy density, with the exception of the 10^3 volume, we see no evidence for a sharpening of the crossover with increasing volume. The quark number susceptibility also shows no apparent trend with increasing volume, as shown in Fig. 10.

IV. SUMMARY AND DISCUSSION

We have extended the equivalence between the QCD-like flux tube model and Potts model to nonzero chemical potential, making possible a direct numerical simulation using standard Monte Carlo methods, where only mean field methods have previously succeeded. We have developed numerical evidence that confirms the predictions of mean field theory, namely that the deconfining phase transition disappears if the baryon density is slightly nonzero. While our results are not applicable in the most interesting limit of small quark mass, one may speculate, nonetheless, that they indicate a weakening of the crossover at high baryon number density.

A recent study by Blum, Hetrick and Toussaint analyzes the static limit of QCD and arrives at a similar conclusion concerning the fate of the deconfining phase transition at high density [12]. Their resulting static action is quite similar to the Potts model action with imaginary magnetic field, so their method is also limited to small volumes in a direct Monte Carlo simulation. To obtain the comparable limit in the flux tube model, one takes $m \to \infty$ with $m - \mu$ fixed. With only two variables, namely $\beta\sigma$ and $\beta(m-\mu)$, one obtains a two-dimensional subspace of the Potts parameter space $(J\beta', h\beta', h'\beta')$. For large $m-\mu$ one has $h = h' \approx 0$, where the first order deconfining transition occurs, whereas at small $m-\mu$ one explores the region of large $h\beta'$ and large $h'\beta'$. In this way the results can be compared.

In the corresponding canonical-ensemble study in the static limit of QCD, a weakening of the crossover signal is also found at nonzero baryon number [13]. However, the authors interpret their results as suggesting the coexistence of two phases in the transition region.

Could a similar change of basis also render full QCD

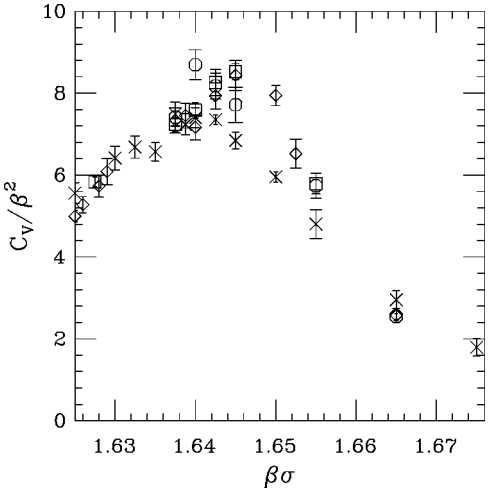

FIG. 8. Specific heat vs $\beta\sigma$ at chemical potential $\beta\mu = 1.75$ for various lattice sizes. Symbols as in Fig. 3.

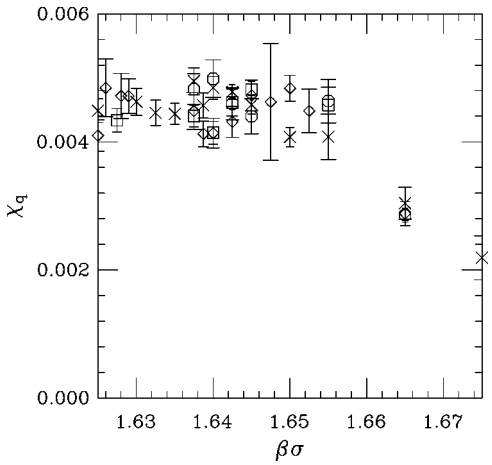

FIG. 10. Quark number susceptibility vs $\beta\sigma$ at chemical potential $\beta\mu = 1.75$ for various lattice sizes. Symbols as in Fig. 3.

simulations tractable at nonzero chemical potential? Normally the QCD path integral is formulated on a basis in which the vector potential is diagonal and the fermion integration is completed explicitly. The analogous change of basis diagonalizes the color electric flux and treats fermions in the Fock space basis, summing over states that are color singlets in quark and gluon content. At finite N_c it appears that the complexities of enforcing color neutrality in such a basis are prohibitive.

ACKNOWLEDGMENTS

We thank Doug Toussaint for helpful comments. Some computations were carried out on the IBM SP at the Utah Center for High Performance Computing.

[1] C. DeTar, Nucl. Phys. B (Proc. Suppl.) **42**, 73 (1995); in *Quark Gluon Plasma 2*, edited by R. Hwa (World Scientific, Singapore, 1995).

[2] For a brief review, see I. Barbour, S. Morrison, E. Klepfish, J. Kogut, and M. Lombardo, Nucl. Phys. B (Proc. Suppl.) **26**, 220 (1998).

[3] L. G. Yaffe and B. Svetitsky, Phys. Rev. D **26**, 963 (1982); A. M. Polyakov, Phys. Lett. **72B**, 477 (1978); L. Susskind, Phys. Rev. D **20**, 2610 (1979).

[4] A. Patel, Nucl. Phys. **B243**, 411 (1984); Phys. Lett. **139B**, 394 (1984).

[5] T. A. DeGrand and C. DeTar, Nucl. Phys. **B225**, 590 (1983).

[6] R. D. Pisarski and F. Wilclzek, Phys. Rev. D **29**, 338 (1992); F. Wilczek, Mod. Phys. Lett. A **7**, 3911 (1992); K. Rajagopal and F. Wilczek, Nucl. Phys. **B399**, 395 (1993); K. Rajagopal, in *Quark Gluon Plasma 2* [1].

[7] C. Bernard *et al.*, Phys. Rev. D **49**, 6051 (1994).

[8] W. Janke and R. Villanova, Nucl. Phys. **B489**, 679 (1997); R. V. Gavai, F. Karsch, and B. Petersson, *ibid.* **B322**, 738 (1989); R. V. Gavai, S. Gupta, A. Irbäck, F. Karsch, and B. Petersson, *ibid.* **B329**, 263 (1990).

[9] R. H. Swendson and J.-S. Wang, Phys. Rev. Lett. **58**, 86 (1987).

[10] R. V. Gavai, F. Karsch, and B. Petersson, Nucl. Phys. **B322**, 738 (1989); R. V. Gavai, S. Gupta, A. Irbäck, F. Karsch, and B. Petersson, *ibid.* **B329**, 263 (1990).

[11] C. Borgs, R. Kotecký, and S. Miracle-Solé, J. Stat. Phys. **62**, 529 (1991).

[12] T. Blum, J. Hetrick, and D. Toussaint, Phys. Rev. Lett. **76**, 1019 (1996).

[13] O. Kaczmarek, J. Engels, F. Karsch, and E. Laermann, ''Lattice QCD at nonzero baryon number,'' hep-lat/9905022; O. Kaczmarek, F. Karsch, E. Laermann, and M. Lutgemeier, ''Heavy quark potentials in quenched QCD at high temperature,'' hep-lat/9908010; J. Engels, O. Kaczmarek, F. Karsch, and E. Laermann, Proceedings of the 17th International Symposium of Lattice Field Theory ''Lattice 99,'' Pisa, Italy, hep-lat/9908046.